Hierarchical Classification and Knowledge-Based Decision Tree for Land Use/Land Cover Classification with Very High Resolution Imagery

Nichols, C., Hung, M.-C., and Wu, Y.-H.
Department of Humanities and Social Science, Northwest Missouri State University, 800 University Drive
Maryville, Missouri, USA
E-mail: mappernick@gmail.com, mhung@nwmissouri.edu, ywu@nwmissouri.edu

Abstract

Very high resolution aerial imagery, while providing a very high level of detail of the land surface, introduced new challenges for land use / land cover (LULC) classification. Finer spatial resolution increases the spectral heterogeneity of the land cover features being classified, and markedly increases the number of shadow pixels. The result is a very large proportion of confused pixels sprinkled throughout the image which adversely affects the accuracy of LULC classification. This paper describes a hierarchical classification approach using knowledge-based decision tree for LULC classification (coniferous, deciduous, bare ground, water, and roads) with a very-high resolution (30cm) multispectral imagery. Shadowed or confused pixels were identified and underwent separate processes to effectively reassign those pixels to the base LULC classes, which was determined by the knowledge-based decision tree in this order: roads, water, coniferous, bare ground, and deciduous based on uniqueness of their spectral reflectance and whether they can be clearly separated from other classes. The overall classification accuracy is 89.4% with a Kappa of 0.85.

1. Introduction

High spatial resolution imagery over forested lands offers land managers special benefits and challenges for land use/land cover (LULC) classification mapping compared to coarser (lower) spatial resolution multispectral imagery (Bauer et al., 1994, Boggs, 2010 and Chubey et al., 2006). Important benefits include the ability to see higher detail and potentially higher classification accuracy. Yet, despite these benefits, challenges include higher intra-class spectral variability and confused pixels that can adversely affect classification accuracy (Yu et al., 2006, Orny et al., 2010, Im and Jensen, 2005 and Sawaya et al., 2003).

Finer (higher) resolution offers the benefit of seeing much higher detail of the land surface which provides sharper, more accurate delineation of LULC boundaries where there are distinctive boundaries between classes such as road edges, field boundaries, buildings, and parking areas. Plus, very-high resolution imagery offers a greater ability to distinguish smaller features such as individual buildings and trees (Gougeon and Leckie, 2006, Hirschmugl et al., 2007, Ke and Quackenbush, 2011 and Pouliot et al., 2002) and small areas of individual vegetation species (Pasher and King, 2009, Ouyang et al., 2011 and Pu and Landry, 2012), whereas pixels in lower resolution imagery average out the spectral reflectance of individual features and vegetation species within each pixel's coverage area. Sawaya et al., (2003) stated that the clarity of high resolution imagery provides far more visual interpretation and assessment than previously possible with lower resolution imagery (such as Landsat). It is essential to have sub-meter very high spatial resolution images to successfully identify and monitor riverside ecosystem influenced by tides (Ehlers et al., 2006), to successfully extract road centerlines (Gao et al., 2018), to successfully identify water features and outline whatershed boundaries (Marcus and Fonstad, 2008), and to successfully assess damages for crisis response (Pesaresi et al., 2010). There are needs of very high resolution remote sensing images to accurately map and monitor our environments for better natural resource management.

However, higher resolution may not improve classification performance and accuracy (Hsieh et al., 2001 and Su et al., 2008). This is because the higher intra-class spectral variability associated with very-high resolution imagery reduces the separability between classes resulting in high pixel classification confusion (a relatively high number of pixels that are not readily assignable to a known LULC class). This is manifested with a "salt-and-pepper" appearance from the confused pixels in the classification results because individual pixels are

classified differently from their neighbors (Hung and Wu, 2005, Yu et al., 2006, Zhou et al., 2009 and Blashke and Strobl, 2001). Orny et al., (2010) found that class boundaries derived from very- high resolution imagery are often poorly defined in forested areas because of the greater heterogeneity of spectral reflectance within the same class, such as the folds, gaps, shadows, and convolutions in a tree canopy, and in the gradual transition areas on the ground from one class to another, such as coniferous to deciduous. Moreover, Im and Jensen (2005) stated that high spatial resolution imagery, unlike moderate or coarse resolution imagery, exhibits high-frequency components with high contrasts (such as shadow pixels) where there are horizontal overlays of objects that protrude above the terrain (e.g. tall trees) caused by off nadir look angles. In this environment, an individual tree has considerable spectral variability (e.g., pixels representing sunlit crown, shaded crown, and the influence of branches) that puts limitations on a single unique spectral signature for tree classification. Likewise, Sawaya et al., (2003) stated that the spatial detail of high resolution imagery is impressive but the spectral-radiometric similarity between certain classes is compounded with the presence of a greater proportion of confused pixels and the greater variability within classes.

Further class confusion occurs in heavily shadowed areas of forests (Adeline et al., 2013, Dare, 2005 and Shahtahmassebi et al., 2013). This is caused by a combination of low sun angle and tall trees that result in long shadows where pixels have very low brightness values. Very low pixel brightness values can make it very difficult to distinguish the LULC type hidden in the shadows because the spectral signatures are so similar between them. When examining spectral reflectance from various land use/cover types, Sawaya et al., (2003) and Hung and Ridd (2002) reported confusion among open water and shadows as dark features, among wetlands, shadows, asphalt, and forest as moderately dark or medium features, and among concrete, bare fields, snow, and salt as bright features. Sugumaran et al., (2003) discovered that in images with 1 m resolution, tree crowns could be identified with a minimum shadow effect. However, in very-high resolution 30 cm images, individual trees are seen more clearly but the resolution is so high that the number and proportion of shadow pixels is also much higher.

The research objective of this study was to develop and test a methodology to achieve a high accuracy (85% or higher) LULC classification accuracy on very-high spatial resolution (30cm) multispectral imagery (Green, Red, NIR (near infrared)) in a forested area. Major challenges for very-high spatial resolution imagery of forested area are shadows and confused classes. The proposed methodology utilizes hierarchical classification and knowledge-based decision tree to overcome shadows and confused classes and identify five land cover classes: coniferous forest, deciduous forest, bare ground, water, and roads with a minimum mapping unit (MMU) of 0.25 acres ($1011m^2$). The .25 acre MMU was chosen for practical purposes because it was the smallest area involved in many land management decisions.

2. Study Area and Data

The 2.32 square kilometer (574 acre) area in the Lake Maumelle watershed within Perry County, Arkansas was an excellent site for this study (Figure 1). A LULC map of the study area can be an aid in resource management, land use planning, surface water runoff management, and timber management. The study area consists of flat to rolling topography with extensive coniferous and deciduous forest. There are a few small lakes, a few cleared areas for agricultural fields, and areas where timber was harvested. The coniferous trees are primarily mature pine, and the deciduous forest is primarily oak and hickory hardwoods. There is very little urban development, and the road network consists of a small number of two-lane asphalt roads, with dirt and gravel access roads into the wooded and harvested timber areas. The Maumelle River curves along the western and southern sides of the study area.

The image for this study is a 30cm (1-foot) February 2009 leaf-off multispectral aerial imagery (Green, Red, and NIR) that included snow cover. The LULC classification accuracy has to be at least 85% as measured from an error matrix table. There are significant heavy tree shadows in the aerial imagery that hide many types of land cover classes over the land on the north side of trees. These shadows are so dark that it is not possible to distinguish the correct land cover class in the shadowed area using a simple image classification approach that is heavily reliant on image-wide spectral reflectance alone. There are also large, mixed, transitional land cover areas between many of the coniferous and deciduous areas.
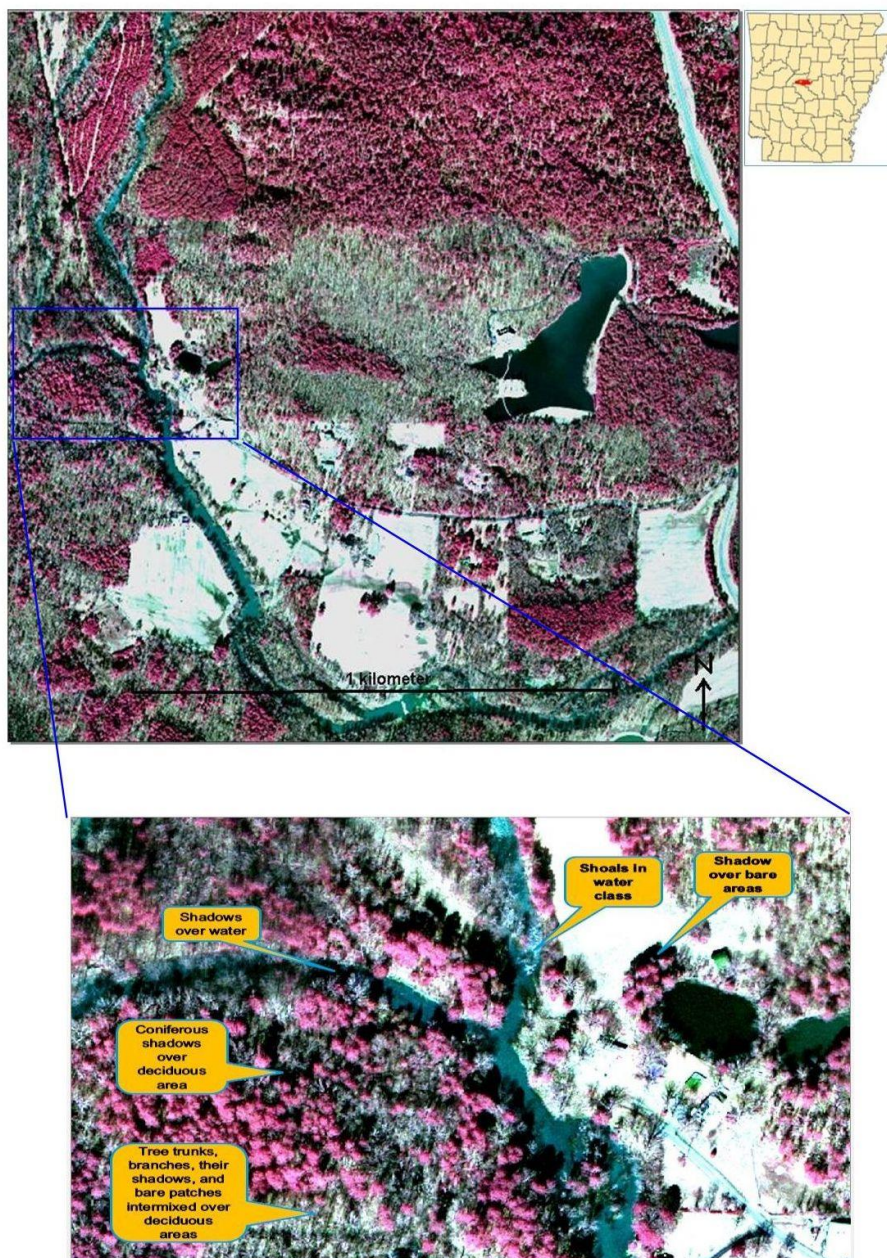
Figure 1: False color aerial photo of the 1.5 x 1.5 km study area

3. General Methodology

The general approach began with ISODATA (Iterative Self-Organizing Data Analysis Technique Algorithm) clustering (Jensen, 2015) as used by Lang (2007), Germaine and Hung (2011) and Sawaya et al., (2003) to create a large number of spectral classes, 100 in this study. After the initial ISODATA unsupervised classification, each of the spectral clusters was assigned (labeled) to a specific land use/cover class using photointerpretation. This aggregated the high number of spectral clusters to the few target land cover classes. This approach

effectively identified and labeled the heterogeneous pixels belonging within each specific land use/cover class; however, there were some spectral clusters that appeared to belong to multiple land use/cover classes (confused pixels) during the labeling process. These clusters had to be segregated into a temporary confused class for subsequent processing.

Distinguishing LULC classes within shadowed areas required more refinement because the image brightness values were so low that the spectral signatures between LULC classes were very similar. So, in a process similar to that used by Ehlers et al.,

(2003), Sawaya et al., (2003) and Germaine and Hung (2011) a separate ISODATA classification/LULC class assignment of just the shadowed areas was performed using the same process described earlier. The result of the re-classified shadow pixels was then added to the initial ISODATA LULC classification. This boosted the number and proportion of classified pixels, and reduced the number and proportion of unclassified pixels (confused).

Each LULC class was then exported as a mask image consisting of two classes - either that particular LULC class or non-such - which enabled further refinement and elimination of small islands of pixels less than the .25 acre MMU within each class. The LULC classes were then combined using hierarchical image stacking. The classes having the highest classification accuracy had priority over those with lower classification accuracy (Figure 2). The LULC classification hierarchy was established empirically by each class's relative classification accuracy as determined by photointerpretation during the ISODATA class assignment process. The following describes the factors that influenced the structure of that hierarchy: roads, water, coniferous, bare ground, and deciduous.
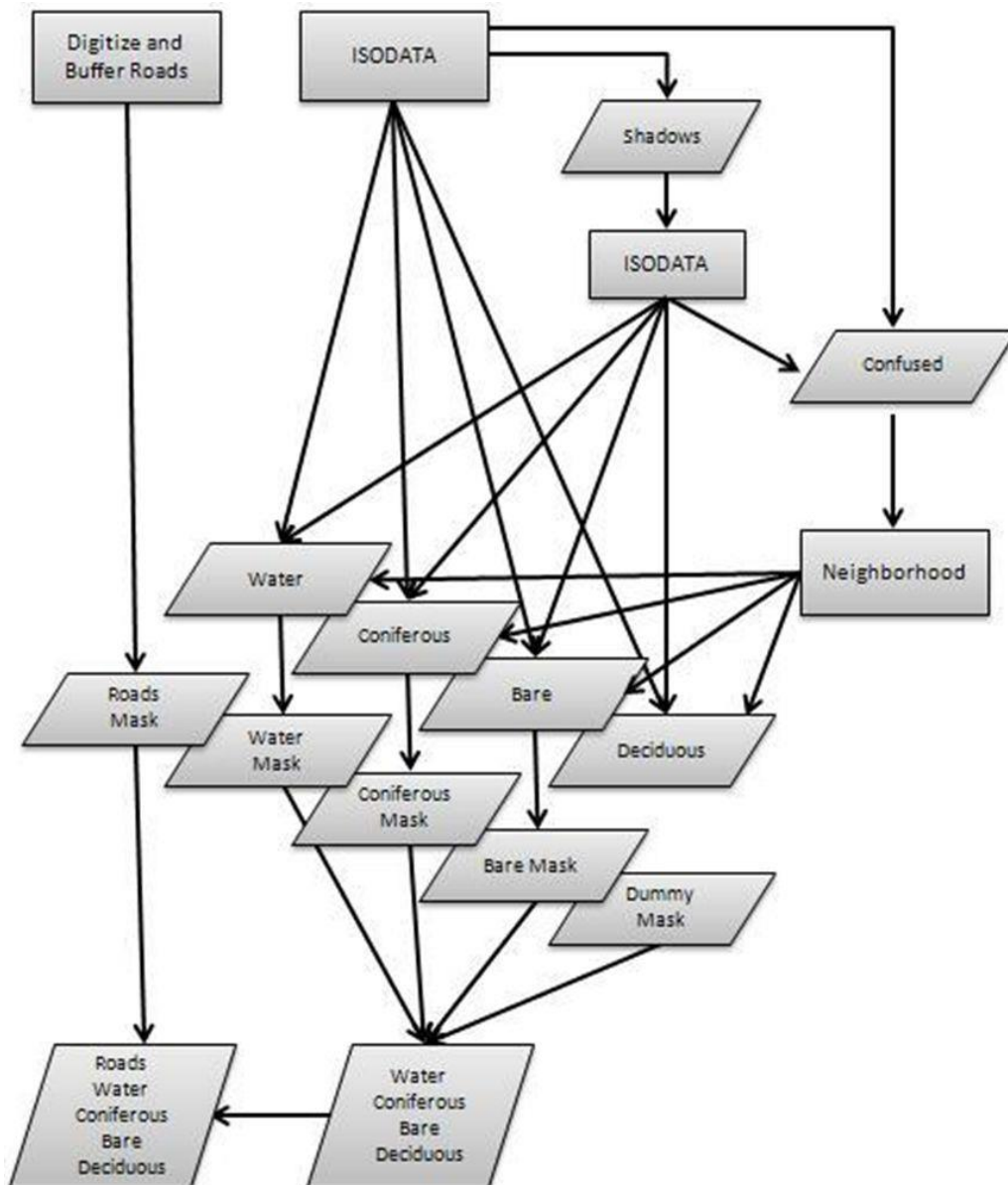

Figure 2: Image classification flowchart

3.1 Establishment of the Classification Hierarchy

Trees, tree shadows, snow, and slush were hiding road pixels so badly that an image processing solution alone would have resulted in considerable classification errors. So, to achieve exceptionally high LULC classification accuracy, road centerlines were easily and quickly digitized as a simple line shapefile off the original very high resolution aerial image based on photointerpretation. Then, a polygon buffer was created around the road centerlines based on the road width as directly measured from the image. The high-accuracy roads were superimposed over the top of all other classes as the last step.

Water pixels were very distinct from other pixels in the image due to the relatively high homogeneity of spectral signatures for water and because its NIR reflectance values were distinctly lower than the other classes (Govender et al., 2007). Thus, based on photo interpretation of the aerial image, water pixels extracted using all three bands in the ISODATA unsupervised classification left an unambiguous distinction of water versus non-water areas.

Coniferous pixels also had very distinct spectral signatures, but they were not as homogeneous as water, since there were internal shadows and folds in the tree canopy to contend with. Living, leafy vegetation reflects NIR light considerably more than other types of land cover (Bauer et al., 1994). In winter, the only large masses of living, leafy vegetation in Arkansas are coniferous. That is why the coniferous vegetation in the aerial photo (displayed in bright red) is so clearly distinguished from other land cover types and why the spectral reflectance is also quite distinct. The effect of coniferous tree shadows adversely affecting the LULC classification was considerable on land cover not of the same height (bare earth and deciduous). However, the effects of shadows on coniferous trees of similar height (other coniferous trees) were considerably less than the bare earth or deciduous land cover classes based on empirical observations from photo-interpretation.

Bare soil was distinct because of the snow cover, but there were a few areas of melted snow and slush that created confusion, and many mixed class transitional areas (smaller bare soil areas interspersed within other classes) also increased the complexity and reduced the accuracy of the bare class compared to water or coniferous classes. The deciduous class would be the most complex and difficult class to accurately extract from the image because the spectral signatures of tree trunks, branches and their shadows, and snow cover often matched those of the other classes. So, a simpler approach was used. First, all the other classes were determined (road, water, coniferous, and bare earth). Thus, all remaining pixels would be deciduous class based on a process of elimination. This approach thus avoids having to do any separate classification of the deciduous class at all.

4. Image Classification

4.1 Initial ISODATA Classification

The first step was to use the Iterative Self-Organizing Data Analysis Technique Algorithm (ISODATA) method of unsupervised classification to generate 100 spectral classes (Jensen, 2015). The geographic location of the pixels associated with each of the 100 spectral classes was visually identified on the original aerial photo. Each spectral class was then recoded to one of six land cover classes – water, coniferous, bare land, deciduous, shadows, and confused – based on visual photo-interpretation. The spectral classes associated with tree shadows needed to be assigned to a temporary tree shadow class since the ground beneath a tree shadow could represent any of several classes (such as roads, water, or bare earth). The spectral classes that were not clearly distinguished as a specific land cover class or tree shadow class were separated out temporarily to a confused pixels class for further processing. Roads were not included in this step since that land cover classification would be superimposed later.

This process effectively and accurately assigned pixels to heterogeneous land classes (Table 1). It was especially apparent, when doing the aggregation, that the pixels at the top of the coniferous trees had spectral characteristics that were quite different from the pixels within the crown folds or the outside edges of the crown. The high spectral heterogeneity within the coniferous class resulted in a large number of spectral classes (28) being coniferous. There was also high spectral heterogeneity within the shadow and confused classes.

Only 3% of the pixels were decidedly deciduous in the initial classification (Table 1 and Figure 3a) even though a casual look at the original aerial photo showed that deciduous obviously covered a considerably larger area. This is because during the photointepretive class aggregation process, a high proportion of candidate deciduous classes appeared to qualify as both deciduous and other classes as well rather than pure deciduous. So, they were assigned as confused pixels instead. The very low percentage of decidedly deciduous pixels was a strong justification for having the deciduous class as the residual class in the hierarchy.

Table 1. Results of initial ISODATA clustering and coding

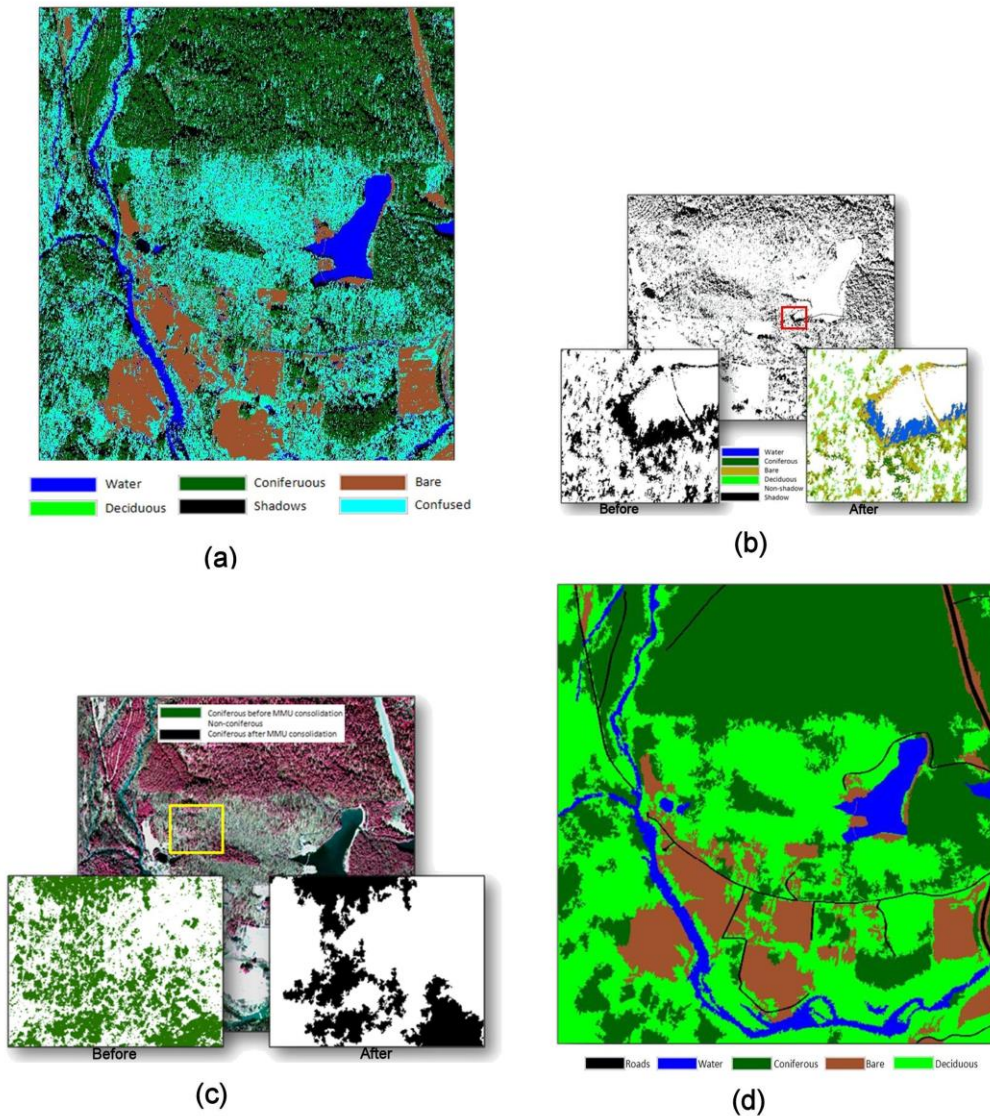| Class	Total Pixels	Percent (%)	# Clusters
Water	1,334,736	5	7
Coniferous	5,427,912	22	28
Bare	3,489,464	14	9
Deciduous	657,295	3	3
Shadows	6,382,812	26	18
Confused	7,712,781	31	35
Total	25,005,000	100	100

Figure 3: Image classification results. (a) Classified image from initial ISODATA. (b) Reclassifying shadows. (c) MMU consolidation. (d) Final classification

Table 2: Results of combining Initial and Shadows-Only ISODATA classification

Class	Initial ISODATA		Shadow ISODATA		Combined	
	Pixels	%	Pixels	%	Pixels	%
Water	1,334,736	5	159,893	3	1,494,629	6
Coniferous	5,427,912	22	2,560,744	40	7,988,656	32
Bare	3,489,464	14		0	3,489,464	14
Deciduous	657,295	3	1,277,280	20	1,934,575	8
Shadows	6,382,812	26		0	-	0
Confused	7,712,781	31	2,384,895	37	10,097,676	40
Total	25,005,000	100	6,382,812	100	25,005,000	100

4.2 Allocate Shadows to the Principal Land Cover Classes

To extract land cover classes from shadows, the first step was to create a mask from the shadow class created in step 1. An ISODATA classification was then performed only on these shadow pixels, and yielded 50 spectral clusters, which were subsequently re-classified to water, coniferous, deciduous, bare ground, and confused using the same photo interpretive techniques used in step 1. This result was then added to the initial ISODATA classification.

The very large proportion of shadow and confused pixels initially represented 57% of the image (Table 1). The shadows alone - exacerbated by the low sun angle - accounted for 26% of the image. This was consistent with past studies regarding the high level of confusion inherent in very-high resolution imagery (Hsieh et al., 2001, Zhou et al., 2009, Ouyang et al., 2011, Adeline et al., 2013 and Boggs, 2010). The proportion of shadow was so high, that a test using a majority filter to reassign the confused and shadow pixels to one of the four land cover classes (water, coniferous, bare, or deciduous) resulted in long strings of contiguous pixels that obviously had little relation to reality. This is because there were not enough "good" LULC pixels (those of a decidedly known class) to provide a solid foundation for successful spatial autocorrelation. Boosting the proportion of "good" pixels by performing a separate ISODATA classification of the shadowed areas (Figure 3b) and adding that result to the initial ISODATA classification remedied the problem. This action boosted the proportion of "good" LULC pixels from only 43% of the image to 60% of the image (Table 2) which was enough to allow the majority filtering process in step 3 to perform. This effectively removed the confusion associated with shadows. No bare pixels resulted from this step because during the photointepretive class aggregation process, the spectral classes over bare land also occurred over other types of land class areas. There were no decidedly "pure" bare pixels. Therefore, these mixed pixels were included in the confused category.

4.3 Allocate Confused Pixels to Land Cover Classes

The neighborhood functionality was used to reassign the confused pixels that were liberally sprinkled throughout the image to one of the four land cover classes (water, coniferous, bare, or deciduous) that they were most likely to belong to based on spatial auto-correlation. Thus, a confused pixel was re-coded according to the predominant land cover class of its immediate neighboring pixels using a 3 x 3 neighborhood majority filter (Germaine and Hung, 2011). It only required three iterations for reassignment of over 99% of the confused pixels to the other classes (Table 3). Since most of the confused pixels were in deciduous areas to begin with, the largest percentage of confused pixels went to deciduous. Roads were not included since that land cover classification would be superimposed later.

4.4 Create Masks of Each Class and MMU Consolidation

It was necessary at this point to remove noise by eliminating the small islands of pixels that were less than the .25 acre MMU (10,890 connected pixels) within and outside of each class (water, coniferous, and bare). This worked best by first creating a mask of each class. A deciduous mask was not necessary because the deciduous class would be determined later by process of elimination. But, it was necessary to create a temporary dummy deciduous mask containing all pixels in the image. The clump and eliminate functions were then consecutively performed to eliminate the small islands of each class's pixels.

Table 3: Results of reassigning confused pixels based on proximate dominant class from each iteration. Numbers are in percent (%)

Class	Beginning	First	Second	Third
Water	6	8	9	9
Coniferous	32	42	44	44
Bare	14	18	18	18
Deciduous	8	24	28	28
Confused	40	8	1	0
Total	100	100	100	100

Eight connected neighbors had slightly better results than using four based on empirical photo interpretive comparisons with the original aerial image. In the bottom left of Figure 3(c), one can see the distribution of the noise throughout the coniferous mask. Performing the clump/eliminate functions effectively eliminated the small islands of pixels. However, the nature of very high spatial resolution imagery introduced an interesting artifact in this process. The ERDAS algorithm simply eliminated areas of less than 10,890 contiguous pixels. Areas larger than that were kept - even if there was a skinny path of pixels one pixel wide connecting two larger areas. So, the result was a highly convoluted class boundary shape. Further smoothing could reduce this, but close visual comparisons with the aerial photo would support the higher LULC accuracy without smoothing, and it better conveys to the map users the mixed nature of the land cover classes in those areas.

4.5 Combine Mask Classes Hierarchically
At this point, the land class masks have some overlaps and gaps with each other that needed to be reconciled. The land cover class layers had different hierarchical levels of inherent classification accuracy. Roads were at the top of the hierarchy, followed by water, coniferous, and bare ground. Since all the other pixels were classified, the remaining pixels would be deciduous by process of elimination. The following piece of pseudo code shows the logic and order of assigning land cover classes to the Combine_Class layer. The first expression that was true determined the final output LULC class for each pixel:

```
If Water_Final == true
    Then Combine_Class = water
Elseif Coniferous_Final == true
    Then Combine_Class = coniferous
Elseif Bare_Final == true
    Then Combine_Class = bare
Else Combine_Class = Deciduous
```

A final clump/eliminate on the results of the Combine_Classes – No Roads model eliminated noise consisting of small islands of pixels less than the .25 acre MMU.

The hierarchical model that combined each of the individual binary LULC masked classes, and through a process of elimination left the deciduous class, was very effective in eliminating the small overlaps and gaps in coverage between the masked classes in a logical manner, and assured that all of the study area was classified. Note that the deciduous class was processed prior to this point the same as water, coniferous, and bare ground even though it was not used in this step. This was to prevent confused and shadow pixels from attaching themselves to water, coniferous, and bare during step 3 in areas known to be deciduous in order to avoid distortions.

4.6 Superimpose Roads
The final step was to superimpose the roads class over the existing LULC classes. The result made roads a particularly accurate land cover class (Figure 3(d)). This simple approach effectively eliminated the need to extract the road class using image processing techniques. The following piece of pseudo code shows the logic and order of assigning final land cover classes:

```
If Road_Final == true Then Final = road
Else Final = Combine_Class
```

5. Accuracy Assessment
A stratified random sampling approach of 216 sample locations was used to test the accuracy of the final LULC classification. Photointerpretation was used over each of the sample locations from the aerial image to determine the appropriate LULC class type. The very high resolution aerial photo displayed the land surface very clearly, so photo-interpretation was justifiable as ground truth verification of the LULC classification.

The final result (Table 4) compares the initial versus the final proportion of pixels belonging to

each land cover class. The original ISODATA classification revealed that 57% of the image had shadow or confused pixels. Now there are no shadows or confused pixels because they were reallocated to the appropriate principal land class types. There was a net increase of pixels to roads because they were superimposed as the last step. The net increase in pixels for water was primarily the conversion of shadow pixels along southern shorelines to the water class. Coniferous pixels increased primarily from the removal of extensive shadows within the canopy. The net decrease in bare pixels was primarily due to the MMU removal of extensive tiny bare areas within the other classes. Deciduous had the highest initial pixel confusion with only 3% decidedly deciduous pixels to start but ended up as 39% of the image. This huge net increase was the result of the hierarchical process of elimination described earlier whereby deciduous was the residual.

Table 5 is an error matrix showing the results of the final LULC classification using the approach described by Congalton and Green (2009). A total accuracy of 89.4% was achieved with a Kappa coefficient of .85. Certain individual classes in the error matrix such as water, coniferous, and bare had user's accuracies above 90% - justifying their high rank in the hierarchal model. However, isolated weaknesses in the classification process occurred where some areas of bare land as seen in the aerial photo were excluded from the bare category (error of omission) and assigned to deciduous instead. Upon visual investigation, some slushy/muddy areas on bare land in the aerial photo were incorrectly classified as deciduous because they had distinctly different spectral characteristics from the rest of the bare class. These slushy/muddy areas were easily found, and could be manually re-classified to bare ground as a touch up to improve the classification accuracy, if necessary. There is high ambiguity where pixels must be clearly assigned to either deciduous or coniferous classes within evenly mixed deciduous/coniferous areas. However, the coniferous/deciduous accuracy results were high because the very high spatial resolution imagery enabled clear distinction of individual coniferous trees from the surrounding area.

Table 4: Initial versus final proportion of pixels belonging to each land cover class

Class	Initial ISODATA		Final LULC		Difference
	Pixels	%	Pixels	%	Pixels
Roads	-	0	387,142	2	387,142
Water	1,334,736	5	1,470,428	6	135,692
Coniferous	5,427,912	22	10,223,861	41	4,795,949
Bare	3,489,464	14	3,123,124	12	(366,340)
Deciduous	657,295	3	9,800,445	39	9,143,150
Shadows	6,382,812	26		0	(6,382,812)
Confused	7,712,781	31		0	(7,712,781)
Total	25,005,000	100	25,005,000	100	

Table 5: Error Matrix of LULC Classification Results

Class Type	Water	Conif	Bare	Decid	Road	Total	User's
Water	21	0	1	1	0	23	91%
Coniferous	0	76	0	6	0	82	93%
Bare	1	0	28	1	0	30	93%
Deciduous	2	4	7	64	0	77	83%
Road	0	0	0	0	4	4	100%
Total	24	80	36	72	4	216	
Producers	88%	95%	78%	89%	100%		89%
Total Accuracy	89.4%						
Kappa Coefficient	.85						

As a result of the auto-correlation and clump/eliminate processing, coniferous tree pixels in close proximity to each other and within an area greater than the 0.25 acre MMU were melted together often creating highly convoluted class boundaries within mixed deciduous/coniferous areas. While one could smooth these convolutions, it may be more beneficial to leave them as they are because they convey to the map reader the mixed nature of the land cover in those areas without having a separate mixed deciduous/coniferous land cover class.

The 0.25 acre MMU requirement, whereby any group of pixels less than 10,890 pixels was removed and assigned to its neighboring class, had some effect on accuracy assessment. For instance, suppose a sampling point happened to fall on a lone coniferous tree in a bare area. The sample could be labeled as coniferous, while the whole area was classified as bare, thus causing a misclassification of the sample point. The benefit of an MMU is that it removes classification noise.

6. Discussion

The timing of the aerial image used for this project was fortunate because there was a uniform blanket of fresh snow on the ground that helped to reduce spectral confusion between classes, except for a few isolated areas of slush/mud where there was melted snow. This is because the spectral characteristics of a uniform blanket of fresh snow are much less variable than the underlying soil, rock, and vegetation cover hidden beneath. This made it easier to distinguish the bare areas from other types of land cover during the ISODATA labeling process, and likely contributed to greater accuracy than may otherwise be expected without the snow. The other advantage of having the aerial image acquired during the winter (leaf-off) was that the spectral characteristics of coniferous trees were conspicuously different from those of other land cover types (Brandtberg, 2007 and Ørka et al., 2010). Further research can determine the limitations of the approach described in this paper under more adverse circumstances such as no snow conditions.

As described earlier, the high spectral heterogeneity of land cover features inherent in very high resolution imagery results in much higher proportions of confused pixels within the image (Gergel et al., 2007, Myint et al., 2011, Orny et al., 2010 and Sawaya et al., 2003). It was learned that successful clump/eliminate process depends on having a high enough proportion of "pure" pixels within the image. Extracting the shadows, classifying the land cover within the shadows

separately, and then adding them back in to the core LULC classification process was an effective means to boost the proportion of "pure" pixels above the threshold needed for successful autocorrelation. However, that threshold was not specifically determined for this paper. Future research on thresholds can define whether autocorrelation for LULC classification is viable for any particular image.

Based on the literature, incorporating additional data into this classification process - such as LiDAR, elevation, and additional images taken on different dates - would likely further improve classification accuracy (Alonzo et al., 2014, Carrão et al., 2008 and Yu et al., 2013). Incorporating images taken on different dates also has the potential to more clearly differentiate the correct land class of confused pixels during the ISODATA labeling process. For instance, leaf-on images could more clearly differentiate between bare soil areas and deciduous areas, while leaf-off images can improve differentiation between coniferous and deciduous areas. Blending these results has the potential to more easily identify, and thus increase the proportion of the "pure" pixels which can improve classification accuracy. Further research can explore the use of multi-temporal, especially leaf-on and leaf-off seasons, imagery on LULC classification and accuracy.

Limitations to this research include the labeling step within the ISODATA unsupervised classification approach, as noted earlier, as it introduces a degree of subjectivity by the analyst who decides which information class to assign a cluster class to. Further research that merges the data-assisted labeling approach (DALA) described by Lang (2007) with the methods described in this paper may offer an automated means, with less subjectivity, to address the increased pixel confusion from heavy tree shadows and the use of very-high spatial resolution imagery. The merging of these approaches may enhance classification accuracy, consistency, and repeatability.

The methodology described in this paper addressed LULC classification of forested areas. However, this methodology can be adapted to other types of land cover as well. For instance, the separate LULC processing of shadows as described in this paper could be modified to include LiDAR surface and elevation information to better differentiate land cover classes within the shadowed areas of buildings in an urban setting, or modified to address different land cover classification types hidden in shadows along the wildland/urban interface used to classify fire hazard risk. The hierarchical classification and decision tree worked

well for this study using five LULC classes in this order: roads, water, coniferous, bare ground, and deciduous. Roads are unique because of narrow and long shape with consistent width. Water is unique because of its distinct spectral reflectance pattern. Deciduous is difficult because of mixture of tree trunks, branches, shadows, and/or ground. Knowing this, this hierarchy and decision tree can be modified to fit other landscapes with close observations and examinations of local materials.

7. Conclusions

This study examined the effect of shadow on very high spatial resolution (30cm) multispectral imagery (Green, Red, NIR) in a forested area, and developed a methodology to overcome the shadow problem to achieve an overall classification accuracy of 89.4% with a Kappa of 0.85 with five classes: coniferous, deciduous, bare ground, water, and roads. The methodology is a combination of hierarchical classification and knowledge-based decision tree. It started with an ISODATA unsupervised classification, which identified land use/cover classes, along with shadow and confused pixels. Shadow pixels went through a secondary ISODATA classification, while confused pixels went through rounds of neighborhood functions. Layers for each land use/cover class were created, and noises or island pixels were removed by the clump/eliminate process in each layer. Layers were then patched back to the final classification image according to a decision-tree in this order: water, coniferous, bare ground, and deciduous. Roads were superimposed to the classification image at the final stage. This methodology successfully classified pixels under shadow to their appropriate land use/cover types, and achieve high classification accuracy. This methodology can easily be adapted to other studies areas as well as other sub-meter very high spatial resolution images.

References

Adeline, K. R. M., Chen, M., Briottet, X., Pang, S. K. and Paparoditis, N., 2013, Shadow Detection in Very High Spatial Resolution Aerial Images: A Comparative Study. *ISPRS Journal of Photogrammetry and Remote Sensing*, Vol. 80, 21-38.

Alonzo, M., Bookhagen, B. and Roberts, D. A., 2014, Urban Tree Species Mapping Using Hyperspectral and Lidar Data Fusion. *Remote Sensing of Environment*, Vol. 148, 70-83.

Bauer, M., Burk, T., Ek, A., Coppin, P., Lime, S., Walsh, T., Walters, K., Belfort, W. and Heinzen, D., 1994, Satellite Inventory of Minnesota Forest Resources. *Photogrammetric Engineering and Remote Sensing*, Vol. 60, 287-298.

Blashke, T. and Strobl, J., 2001, What's Wrong with Pixels? Some Recent Developments Interfacing Remote Sensing and GIS. *GeoBIT/GIS*, Vol. 6, 12-17.

Boggs, G. S., 2010, Assessment of SPOT 5 and QuickBird Remotely Sensed Imagery for Mapping Tree Cover in Savannas. *International Journal of Applied Earth Observation and Geoinformation*, Vol. 12(4), 217-224.

Brandtberg, T., 2007, Classifying Individual Tree Species Under Leaf-Off and Leaf-On Conditions Using Airborne Lidar. *ISPRS Journal of Photogrammetry and Remote Sensing*, Vol. 61(5), 325-340.

Carrão, H., Gonçalves, P. and Caetano, M., 2008, Contribution of Multispectral and Multitemporal Information from MODIS Images to Land Cover Classification. *Remote Sensing of Environment*, Vol. 112(3), 986-997.

Chubey, M. S., Franklin, S. E. and Wulder, M. A., 2006, Object-Based Analysis of Ikonos-2 Imagery for Extraction of Forest Inventory Parameters. *Photogrammetric Engineering & Remote Sensing*, Vol. 72(4), 383-394.

Congalton, R. and Green, K., 2009, *Assessing the Accuracy of Remotely Sensed Data.* 2nd ed. Boka Ratan, FL.: CRC Press.

Dare, P., 2005, Shadow Analysis in High-Resolution Satellite Imagery of Urban Areas. *Photogrammetric Engineering and Remote Sensing*. Vol. 71(2), 169-177.

Ehlers, M., Gahler, M. and Janowsky, R., 2003, Automated Analysis of Ultra-High Resolution, Remote Sensing Data for Biotope Type Mapping: New Possibilities and Challenges, *ISPRS Journal of Photogrammetry and Remote Sensing,* Vol. 57(5-6), 315-326.

Ehlers, M., Gaehler, M. and Janowsky, R., 2006, Automated Techniques for Environmental Monitoring and Change Analyses for Ultra High Resolution Remote Sensing Data. *Photogrammetric Engineering and Remote Sensing*, Vol. 72(7), 835-844.

Gao, L., Shi, W., Miao, Z. and Lv, Z., 2018, Method Based on Edge Constraint and Fast Marching for Road Centerline Extraction from Very High-Resolution Remote Sensing Images. *Remote Sensing*, Vol. 10(6), 900. DOI: 10.3390/rs10060900.

Gergel, S. E., Stange, Y., Coops, N. C., Johansen, K. and Kirby, K. R., 2007, What is the Value of a Good Map? An Example Using High Spatial Resolution Imagery to Aid Riparian Restoration. *Ecosystems*, Vol. 10(5), 688-702.

Germaine, K. and Hung, M., 2011, Delineation of Impervious Surface from Multispectral Imagery and LiDAR Incorporating Knowledge-Based Expert System Rules. *Photogrammetric Engineering and Remote Sensing*, Vol. 77(1), 75-85.

Gougeon, F. A. and Leckie, D. G., 2006, The Individual Tree Crown Approach Applied to Ikonos Images of a Coniferous Plantation Area. *Photogrammetric Engineering and Remote Sensing*, Vol. 72(11), 1287-1297.

Govender, M., Chetty, K. and Bulcock, H., 2007, A Review of Hyperspectral Remote Sensing and Its Application in Vegetation and Water Resource Studies. *Water SA Manuscript,* Vol. *33(2).* DOI: 10.4314/wsa.v33i2.49049.

Hirschmugl, M., Ofner, M., Raggam, J. and Schardt, M., 2007, Single Tree Detection in Very High Resolution Remote Sensing Data. *Remote Sensing of Environment*, Vol. 110(4), 533-544.

Hsieh, P., Lee, L. and Chen, L., 2001, Effect of Spatial Resolution on Classification Errors of Pure and Mixed Pixels in Remote Sensing. *IEEE Transactions on Geoscience and Remote Sensing*, Vol. 39(12), 2657-2663.

Hung, M.-C. and Ridd, M. K., 2002, A Sub-pixel Classifier for Urban Land Cover Mapping Based on a Maximum Likelihood Approach and Expert System Rules, *Photogrammetric Engineering and Remote Sensing*, Vol. 68(11), 1173-1180.

Hung, M. and Wu, Y., 2005, Mapping and Visualizing the Great Salt Lake Landscape Dynamics Using Multi-temporal Satellite Images, 1972-1996. *International Journal of Remote Sensing,* Vol. 26(9), 1815-1834.

Im, J. and Jensen, J. R., 2005, A Change Detection Model Based on Neighborhood Correlation Image Analysis and decision Tree Classification. *Remote Sensing of Environment,* Vol. 99 (3), 326-340.

Jensen, J. R., 2015, *Introductory Digital Image Processing: A Remote Sensing Perspective*. 4th ed. Englewood Cliffs, NJ: Prentice-Hall, Inc.

Ke, Y. and Quackenbush, L. J., 2011, A Review of Methods for Automatic Individual Tree-Crown Detection and Delineation From Passive Remote Sensing. *International Journal of Remote Sensing*, Vol. 32(17), 4725-4747.

Lang, R., 2007, Optimizing Unsupervised Classifications of Remotely Sensed Imagery with a Data-Assisted Labeling Approach, *Computers and Geosciences,* Vol. 34, 1877-1885.

Marcus, W. A. and Fonstad, M. A., 2008, Optical Remote Mapping of Rivers at Sub‐Meter Resolutions and Watershed Extents. *Earth Surface Processes and Landforms: The Journal of the British Geomorphological Research Group*, Vol. 33(1), 4-24.

Myint, S. W., Gober, P., Brazel, A., Grossman-Clarke, S. and Weng, Q., 2011, Per-pixel vs. Object-Based Classification of Urban Land Cover Extraction Using High Spatial Resolution Imagery. *Remote Sensing of Environment*, Vol. 115(5), 1145-1161.

Ørka, H. O., Næsset, E. and Bollandsås, O. M., 2010, Effects of Different Sensors and Leaf-On and Leaf-Off Canopy Conditions on Echo Distributions and Individual Tree Properties Derived from Airborne Laser Scanning. *Remote Sensing of Environment*, Vol. 114(7), 1445-1461.

Orny, C., Chehata, N., Boukir, S. and Guyon, D., 2010, Characterization of Maritime Pine Forest Structure Changes with VHR Satellite Imagery: Application to the 24th January 2009 Windfall Damages Cartography. *CNES Technical Report*. 1-24.

Ouyang, Z., Zhang, M., Xie, X., Shen, Q., Guo, H. and Zhao, B., 2011, A Comparison of Pixel-Based and Object-Oriented Approaches to VHR Imagery for Mapping Salt Marsh Plants. *Ecological Informatics*, Vol. 6, 136-146.

Pasher, J. and King, D. J., 2009, Mapping Deadwood Distribution in a Temperate Hardwood Forest Using High Resolution Airborne Imagery. *Forest Ecology and Management*, Vol. 258(7), 1536-1548.

Pesaresi, M., Kemper, T., Gueguen, L. and Soille, P., 2010, Automatic Information Retrieval from Meter and Sub-Meter Resolution Satellite Image Data in Support to Crisis Management. In 2010 *IEEE International Geoscience and Remote Sensing Symposium*, IEEE. 1792-1795.

Pouliot, D. A., King, D. J., Bell, F. W. and Pitt, D. G., 2002, Automated Tree Crown Detection and Delineation in High-Resolution Digital Camera Imagery of Coniferous Forest Regeneration. *Remote Sensing of Environment*, Vol. 82(2-3), 322-334.

Pu, R. and Landry, S., 2012, A Comparative Analysis of High Spatial Resolution IKONOS and WorldView-2 Imagery for Mapping Urban Tree Species. *Remote Sensing of Environment*, Vol. 124, 516-533.

Sawaya, K. E., Olmanson, L. G., Heinert, N., Brezonik, P. L. and Bauer, M. E., 2003, Extending Satellite Remote Sensing to Local Scales: Land and Water Resource Monitoring Using High-Resolution Imagery. *Remote Sensing of Environment*, Vol. 88, 144-156.

Shahtahmassebi, A., Yang, N., Wang, K., Moore, N. and Shen, Z., 2013, Review of Shadow Detection and De-Shadowing Methods in Remote Sensing. *Chinese Geographical Science*, Vol. 23(4), 403-420.

Su, W., Li, J., Chen, Y., Zhigang, L., Zhang, J., Low, T., Suppiah, J. and Hashim, S., 2008, Textural and Local Spatial Statistics for the Object-Oriented Classification of Urban Areas Using High Resolution Imagery. *International Journal of Remote Sensing*, Vol. 29(11), 3105-3117.

Sugumaran, R., Pavuluri M. and Zerr, D., 2003, The Use of High-Resolution Imagery for Identification of Urban Climax Forest Species Using Traditional and Rule-Based Classification Approach. *IEEE Transactions on Geoscience and Remote Sensing*. Vol. 41(9), 1933-1939.

Yu, L., Wang, J. and Gong, P., 2013, Improving 30m Global Land-Cover Map FROM-GLC with Time Series MODIS and Auxiliary Data Sets: A Segmentation-Based Approach. *International Journal of Remote Sensing*, Vol. 34(16), 5851-5867.

Yu, Q., Gong, P., Clinton, N., Biging, G., Kelly, M. and Schirokauer, D., 2006, Object-Based Detailed Vegetation Classification was Airborne High Spatial Resolution, Remote Sensing Imagery. *Photogrammetric Engineering and Remote Sensing,* Vol. 72(7), 799-811.

Zhou, W., Huang, G., Troy, A. and Cadenasso, M. L., 2009, Object-Based Land Cover Classification of Shaded Areas in High Spatial Resolution Imagery of Urban Areas: A Comparison Study. *Remote Sensing of Environment*, Vol. 113(8), 1769-1777.